

Supplementary Information

Nutrient supply controls the linkage between species abundance and ecological interactions in marine bacterial communities

Tianjiao Dai^{1,2}, Donghui Wen^{2*}, Colin T. Bates³, Linwei Wu³, Xue Guo¹, Suo Liu¹,
Yifan Su¹, Jiesi Lei¹, Jizhong Zhou^{3,4,5}, and Yunfeng Yang^{1*}

¹State Key Joint Laboratory of Environment Simulation and Pollution Control, School of Environment, Tsinghua University, Beijing, China

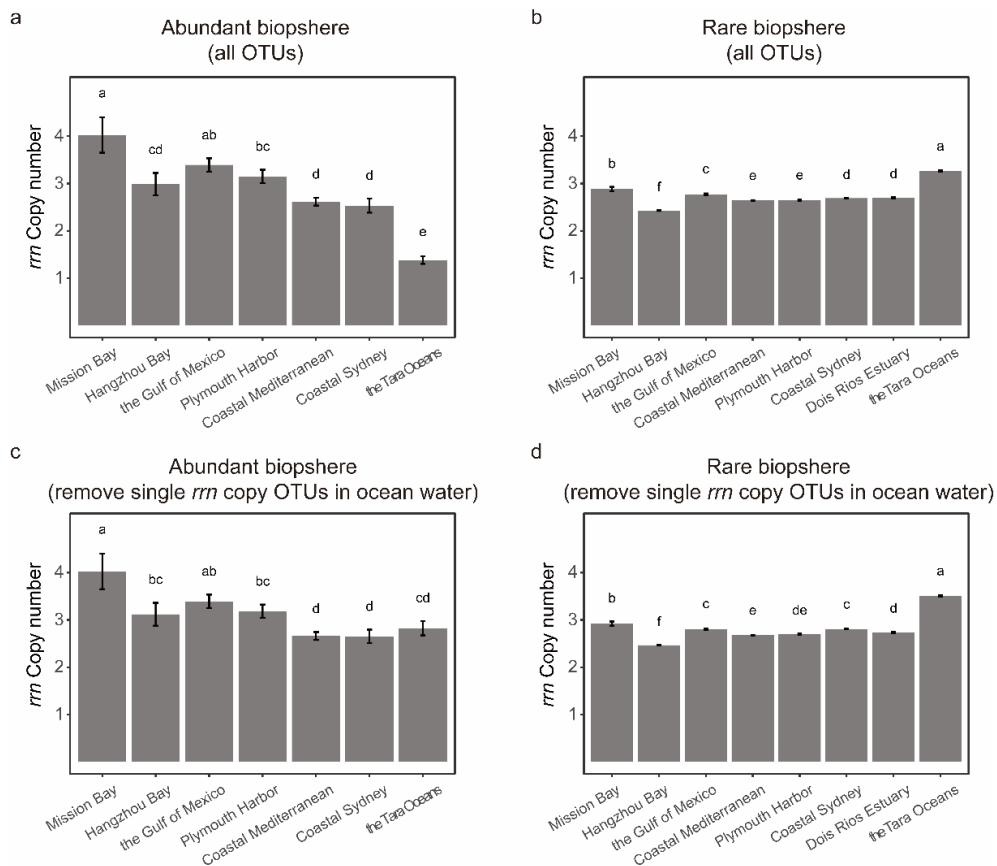
²College of Environmental Sciences and Engineering, Peking University, Beijing 100871, China

³Institute for Environmental Genomics and Department of Microbiology and Plant Biology, University of Oklahoma, Norman, Oklahoma

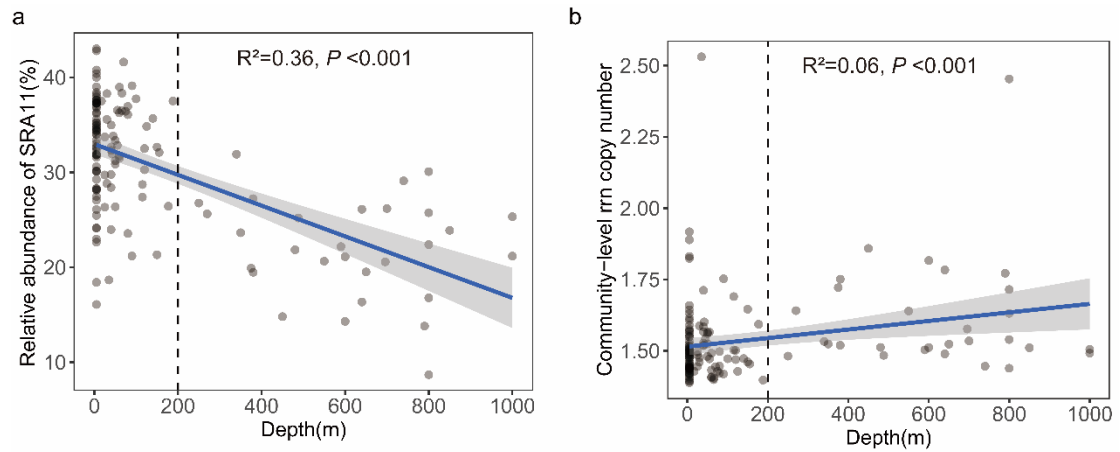
⁴School of Civil Engineering and Environmental Sciences, University of Oklahoma, Norman, OK, USA

⁵Earth and Environmental Sciences, Lawrence Berkeley National Laboratory, Berkeley, California

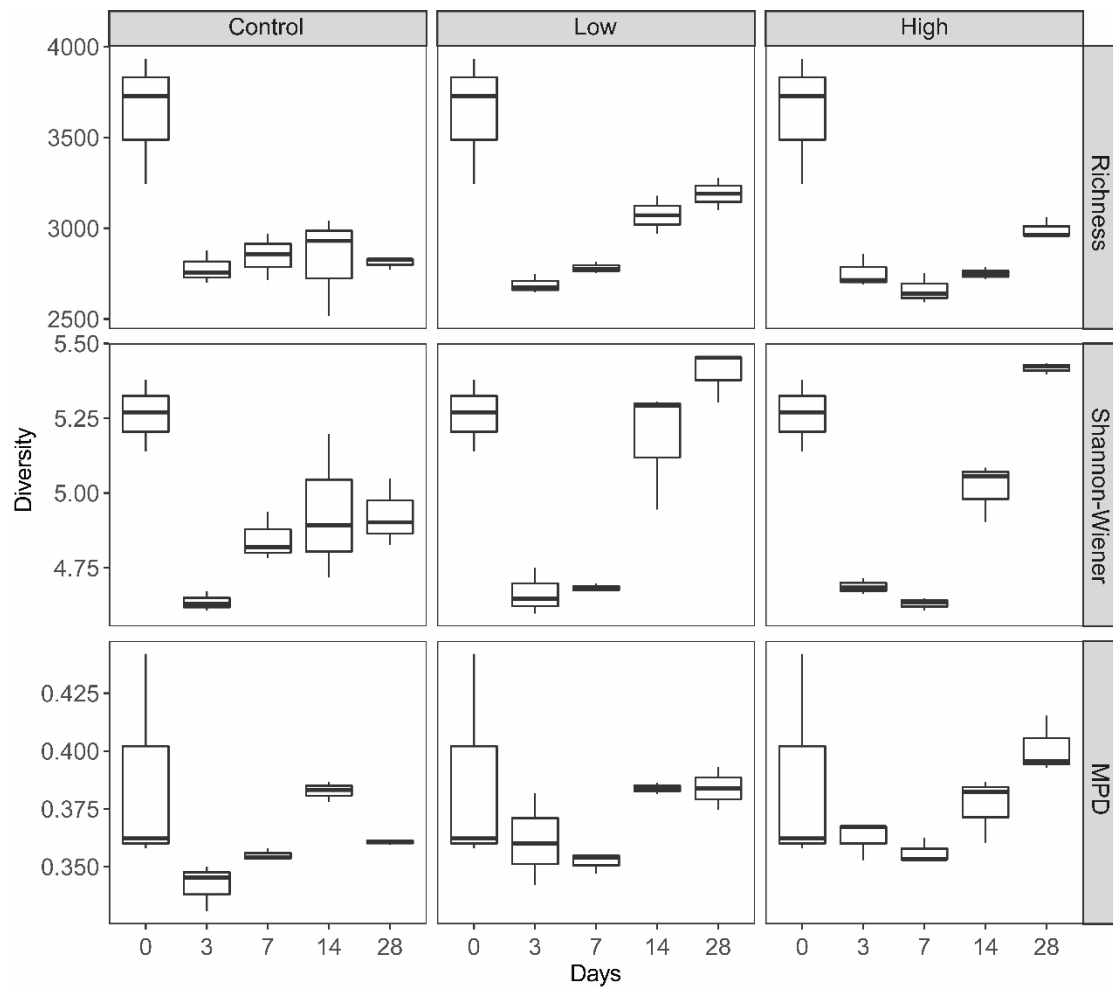
*To whom correspondence may be addressed. Email: dhwen@pku.edu.cn; Tel & Fax: +86-010-62751923; and yangyf@tsinghua.edu.cn; Tel: +86-010-62784692; Fax: +86-010-62794006;



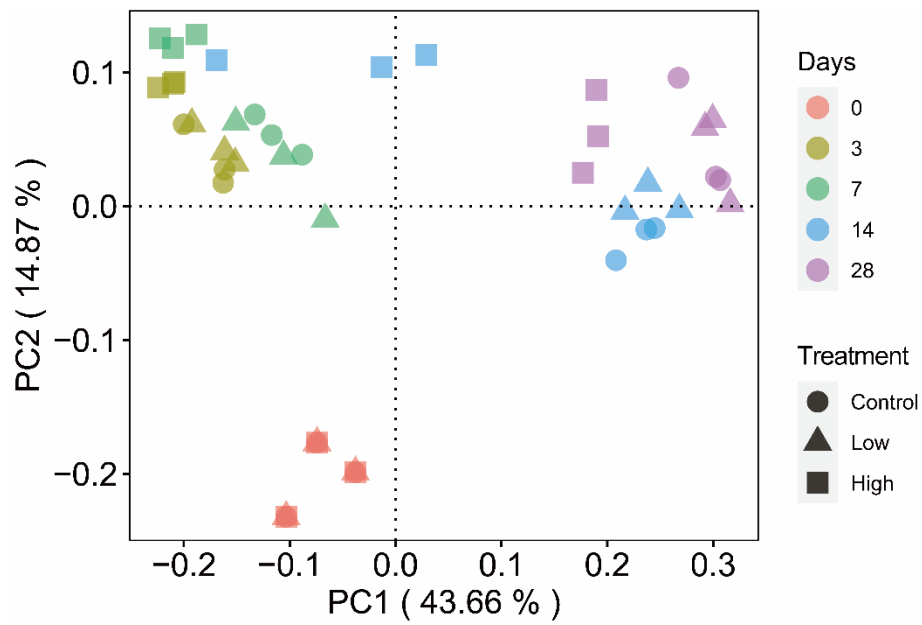
Supplementary Figure 1 The *rrn* copy numbers of abundant and rare biosphere OTUs. All OTUs are included in panels **a** and **b**, while OTUs with a single *rrn* copy in the ocean water dataset are removed in panels **c** and **d**. Bars represent mean values, error bars represent the standard errors, and lowercase letters above the bars indicate significant differences based on one-way ANOVA followed by LSD test (adjusted $P < 0.05$ by Bonferroni method). The sample sizes are listed in Supplementary Table 1. In panels **a** and **c**, the bar representing Dois Rios estuary is missed because no OTU in the dataset was classified as abundant biosphere based on the criteria we defined.



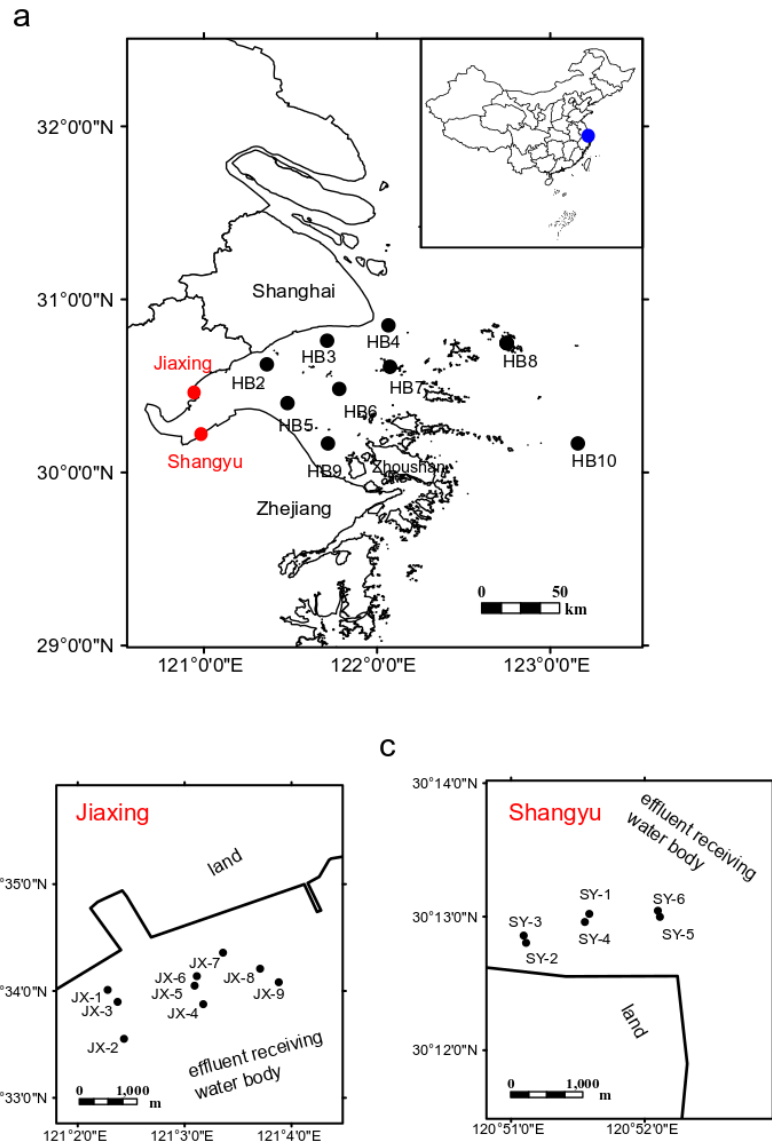
Supplementary Figure 2 The relative abundance of SAR11 and the community community-level *rrn* copy number from the surface to the deep ocean. The dashed lines in **a** and **b** divide the surface ocean (0 - 200 m) and the deep ocean (200 - 1000 m). Adjusted R^2 and P values from linear regression (blue line) are shown together with 95% confidence intervals (gray region).



Supplementary Figure 3 Dynamics of bacterial communities' taxonomic (measured by richness and Shannon-Weiner index) and phylogenetic (measured by mean pairwise distance, MPD) diversity in response to different nutrient supplies. In the boxplots, hinges indicate the 25th, 50th, and 75th percentiles, whiskers indicate $1.5 \times$ interquartile ranges ($n = 3$ biologically independent samples).



Supplementary Figure 4 Principle coordinates ordination based on Bray-Curtis distances showing changes in bacterial community composition by different nutrient supplies.



Supplementary Figure 5 Sampling sites in coastal Hangzhou Bay, China. a, sampling sites inner Hangzhou Bay (HB). **b** and **c**, sampling sites in the coastal wastewater receiving area near Jiaxing City (JX) and Shangyu City (SY).

Supplementary Table 1 The *rrn* copy numbers of the OTUs belonging to abundant, intermediate, and rare biospheres.

Datasets	No. of Samples	No. of OTUs	^a <i>rrn</i> copy number (OTUs %)			
			Abundant	Intermediate	Rare	^b Overall
<i>Coastal sediment</i>						
Mission Bay	20	1759	4.02±0.37 a (n = 11)	3.01±0.06 b (n = 668)	2.88±0.04 b (n = 1080)	2.89±0.09 a
Hangzhou Bay	72	14424	2.99±0.24 a (n = 48)	2.61±0.04 b (n = 1344)	2.43±0.01 c (n = 13032)	2.18±0.01 d
the Gulf of Mexico	6	5839	3.39±0.14 a (n = 86)	3.07±0.05 b (n = 654)	2.77±0.02 c (n = 5153)	2.51±0.01 b
Plymouth Harbor	65	21225	3.15±0.14 a (n = 62)	2.97±0.04 a (n = 1289)	2.64±0.01 b (n = 19874)	2.45±0.02 b
Coastal Mediterranean	11	7343	2.62±0.08 b (n = 123)	2.80±0.06 a (n = 527)	2.65±0.01 b (n = 6693)	2.34±0.01 c
Coastal Sydney	60	89355	2.53±0.15 a (n = 42)	2.72±0.03 a (n = 1291)	2.69±0.01 a (n = 88022)	2.24±0.01 d

	Dois Rios Estuary	9	6500	NA (n = 0)	2.82±0.04 a (n = 987)	2.70±0.02 b (n = 5513)	2.26±0.07 cd
<i>Ocean water</i>	the <i>Tara</i> Oceans	139	26961	1.38±0.07 c (n = 105)	2.93±0.04 b (n = 2445)	3.26±0.01 a (n = 24411)	2.18±0.01 d

^athe *rrn* copy numbers of OTUs are presented as mean ± s.e., where lowercase letters in bold indicate significant difference based on one-way ANOVA followed by LSD test, and data in the brackets indicate the proportion of OTUs in the dataset.

^bthe average *rrn* copy number of all OTUs in a community, i.e., the abundance unweighted community-level average *rrn* copy number.

Supplementary Table 2 Pearson's correlation (two-sided) between environmental nutrients and the community-level *rrn* copy number.

Nutrients	Overall		Abundant		Intermediate		Rare	
	r	<i>P</i>	r	<i>P</i>	r	<i>P</i>	r	<i>P</i>
Hangzhou Bay, China								
^a Ammonia (mg/L)	0.508	<0.001	0.523	<0.001	0.404	0.001	0.300	0.018
^a Phosphate (mg/L)	0.410	0.001	0.432	0.001	0.251	0.052	0.128	0.356
^b Total phosphorus (mg/kg)	0.491	<0.001	0.513	<0.001	0.357	0.004	0.198	0.143
Coastal Sydney								
^b TOC (mg/g)	0.765	<0.001	0.532	<0.001	0.737	<0.001	0.707	<0.001
^b TN (%)	0.779	<0.001	0.542	<0.001	0.734	<0.001	0.754	<0.001
Coastal Mediterranean								
^b Silt and clay (%)	0.782	0.013	0.803	0.013	0.704	0.023	-0.732	0.021
the Tara Oceans								
^a Phosphate (μmol/L)	0.635	<0.001	0.317	<0.001	0.488	<0.001	0.518	<0.001
^a Nitrate and Nitrite (μmol/L)	0.643	<0.001	0.272	0.002	0.489	<0.001	0.499	<0.001

^ameasured for water;

^bmeasured for sediment.

Supplementary Table 3 Effect of nutrient availability and phylogenetic structure on community-level *rrn* copy number by partial Mantel test^a.

Datasets		Nutrients		Phylogenetic structure	
		<i>r</i>	<i>P</i>	<i>r</i>	<i>P</i>
<i>Coastal sediment</i>	Hangzhou Bay, China	0.220	0.026	0.751	0.001
	Coastal Sydney	0.406	0.001	0.266	0.001
	Coastal Mediterranean	0.602	0.001	-0.229	0.947
<i>Ocean water</i>	the Tara Oceans	0.130	0.029	0.483	0.001

^aChanges in the phylogenetic structure are measured by weighted Unifrac distance, and changes in nutrients availability are measured by Euclidean distance. The statistics were derived from partial Mantel test based on two-sided Pearson's correlation.

Supplementary Table 4 Topological features of bacterial communities' association networks in the coastal sediments and global ocean water.

Topological properties	Hangzhou Bay	Plymouth	Coastal Sydney	the Tara Oceans
Correlation coefficient cutoff	0.87	0.89	0.89	0.88
No. of nodes	368	262	485	1158
No. of links	530	514	869	7217
Negative links (%)	31.13	80.35	14.38	0.04
R ² of power-law	0.959	0.828	0.945	0.829
Average degree	2.88	3.924	3.583	12.465
Average clustering coefficient	0.371 (0.147±0.019) ^a	0.114 (0.111±0.020)	0.223 (0.139±0.016)	0.657 (0.589±0.006)
Average path length (avgGD)	8.08 (4.894±0.149)	3.566 (3.596±0.064)	6.104 (4.656±0.192)	4.052 (4.485±0.097)
Transitivity	0.337 (0.137±0.015)	0.064 (0.054±0.007)	0.229 (0.167±0.010)	0.554 (0.526±0.003)

Modularity	0.841	0.587	0.68	0.755
	(0.703±0.015)	(0.524±0.010)	(0.578±0.015)	(0.707±0.004)

^aData in the brackets represent the topological properties of 100 random networks (mean ± sd), which were generated by rewiring all the links with the identical numbers of nodes and links to the corresponding empirical network.

Supplementary Table 5 Quantitative effects of nutrients supply, succession time, and their interactions on the microcosm bacterial community variations by permutational multivariate analysis of variance (adonis)^a.

Source of Variation	Levels	F.Model	R ²	P
Time (Days)	0, 3, 7, 14, 28	14.827	0.153	0.001
	Control			
Nutrients	Low	4.598	0.095	0.001
	High			
Time*Nutrients		1.801	0.037	0.046

^aPermutational multivariate analysis of variance (adonis) was based on Bray-Curtis dissimilarity distance. The two-way ANOVA model was set as dissimilarity ~ nutrients × time using function *adonis* in the R package “*vegan*”.

Supplementary Table 6 Classifications of bacterial OTUs in the microcosm experiments.

Treatment	Total OTUs	Abundant	Intermediate	Rare
Control	10334	75	156	10103
Low	10719	74	163	10482
High	10418	88	148	10182

Supplementary Table 7 Pearson's correlation (two-sided) between nutrient concentrations and community-level *rrn* copy number in the microcosm experiment.

Treatments	Ammonia		Phosphate	
	<i>r</i>	<i>P</i>	<i>r</i>	<i>P</i>
Control	0.616	0.033	0.397	0.201
Low	0.718	0.009	0.614	0.034
High	0.865	< 0.001	0.878	<0.001

Supplementary Table 8 Topological features of microcosm bacterial association networks.

Topological properties	Control	Low	High
Correlation coefficient cutoff	0.913	0.910	0.898
No. of nodes	1036	1301	1328
No. of links	1392	3797	2188
R ² of power-law	0.961	0.903	0.935
Average degree	2.687	5.837	3.295
Average clustering coefficient	0.156 (0.105±0.0) ^a	0.194 (0.173±0.004)	0.130 (0.102±0.00)
Average path length	7.132 (6.502±0.1)	5.834 (5.381±0.134)	7.798 (6.778±0.12)
Transitivity	0.237 (0.165±0.0)	0.338 (0.307±0.003)	0.280 (0.225±0.00)
Modularity	0.784 (0.746±0.0)	0.551 (0.496±0.010)	0.737 (0.701±0.00)

^aData in the brackets represent the topological properties of 100 random networks (mean ± sd), which were generated by rewiring all the links with the identical numbers of nodes and links to the corresponding empirical network.

Supplementary Table 9 Proportion of negative associations in networks for microcosm bacterial communities^a.

Association pairs	Control	Low	High
Abundant - Abundant	33.3% (60)	45.7% (129)	51.5% (101)
Intermediate - Intermediate	46.4% (28)	37.9% (140)	49.1% (57)
Rare - Rare	71.4% (840)	60.7% (1790)	73.6% (1306)
Abundant - Intermediate	42.3% (71)	43.3% (298)	46.2% (119)
Abundant - Rare	44.3% (192)	46.6% (672)	49.0% (304)
Intermediate - Rare	39.3% (201)	43.5% (768)	46.2% (301)

^aThe proportion of negative associations was calculated as negative links/total links that identified for each association pairs in the network, and the data in bracket indicates the absolute number of total links.